EUROPEAN COOPERATION
IN SCIENCE
AND TECHNOLOGY

EURO-COST

CA20120 TD(22)01066
Bologna, Italy
February 8-11, 2022

SOURCE: Universidad Politécnica de Cartagena, Spain
University of Lisbon, Portugal
Universitat Politècnica de Valencia, Spain
Jagiellonian University Medical College, Poland
RWTH Aachen University, Germany
AGH University of Science and Technology, Poland

When Body Area Network Reaches the Nano Level: An Architecture for Cardiovascular Health Applications

Rafael Asorey-Cacheda, Luis M. Correia, Concepcion Garcia-Pardo, Krzysztof Wojcik, Kenan Turbic, and Pawel Kulakowski

Corresponding author:
Pawel Kulakowski
Institute of Telecommunications
AGH University of Science and Technology
Poland
Phone: +48 12 617 3967
Email: kulakowski@agh.edu.pl

When Body Area Network Reaches the Nano Level: An Architecture for Cardiovascular Health Applications

Rafael Asorey-Cacheda, *Member, IEEE*, Luis M. Correia, *Senior Member, IEEE*, Concepcion Garcia-Pardo, Krzysztof Wojcik, Kenan Turbic, *Member, IEEE*, and Pawel Kulakowski

***Abstract*—Cardiovascular events occurring in the bloodstream are responsible for about 40% of human deaths in developed countries. Motivated by this fact, we present a new global network architecture for a system for the diagnosis and treatment of cardiovascular events, focusing on problems related to pulmonary artery occlusion, i.e., situations of artery blockage by a blood clot. The proposed system is based on bio-sensors for detection of artery blockage and bio-actuators for releasing appropriate medicines, both types of devices being implanted in pulmonary arteries. The system can be used by a person leading an active life and provides bidirectional communication with medical personnel via nano-nodes circulating in the bloodstream constituting an in-body area network. We derive an analytical model for calculating the required number of nano-nodes to detect artery blockage and the probability of activating a bio-actuator. We also analyze the performance of the body area component of the system in terms of path loss and of wireless links budget. Results show that the system can diagnose a blocked artery in about 3 hours and that after around 3 hours medicines can be released in the exact spot of the artery occlusion, while with current medical practices the average time for diagnosis varies between 5 to 9 days.**

***Index Terms*—Body Area Networks, Flow-Guided Nano-Networks, IoT for Health, Medical Applications, Nano-Communications, THz Communications.**

R. Asorey-Cacheda is with the Department of Information and Communication Technologies, Universidad Politécnica de Cartagena, 30202 Spain (e-mail: rafael.asorey@upct.es)

L.M. Correia is with IST/INESC-ID, University of Lisbon, Lisbon, Portugal (e-mail: luis.m.correia@tecnico.ulisboa.pt)

C. Garcia-Pardo is with the Institute of Telecommunications and Multimmedia Applications (iTEAM), Universitat Politècnica de Valencia (UPV), 46022 Valencia, Spain (e-mail: cgpardo@iteam.upv.es)

K. Wojcik is with 2nd Department of Internal Medicine, Faculty of Medicine, Jagiellonian University Medical College, Kraków, Poland (e-mail: krzysztof.wojcik@uj.edu.pl)

K. Turbic is with the Institute for Communication Technologies and Embedded Systems (ICE), RWTH Aachen University, Kopernikusstraße 16, 52074 Aachen (e-mail: turbic@ice.rwth-aachen.de)

P. Kulakowski (corresponding author) is with the Institute of Telecommunications, AGH University of Science and Technology, Krakow, Poland (e-mail: kulakowski@agh.edu.pl)

I. Introduction

COMMUNICATION by humans has been considered in the last decades as mobile and wireless communications, i.e., enabling users to communicate with other people, to have access to information, e.g., downloading files, and more recently to present information, e.g., usage of social media. This type of communications has been focused on using a mobile phone as a terminal, where users take action to exchange information. Nevertheless, it is clear that mobile phones will no longer be the preferred terminals of the future, spectacles being an alternative (from the very first Google Glasses [1] to recent RayBan/Facebook ones [2], at the time of writing this paper), and wearable devices in general presenting themselves as a trend to be explored. Moreover, in the last years, the Internet of Things (IoT) has emerged as a new perspective to communications, putting machines communicating with each other, for the benefit of people, via a variety of terminals, such as sensors and actuators, without user's intervention. 5G (the fifth generation of mobile cellular communications systems) is definitely taking a step into this direction, by enabling machine based services that were not possible up to the previous generation. Massive Machine Type Communications (MMTC) are a clear example, as are Ultra Reliable Low Latency Communications (URLLC).

Body Area Networks (BANs) have been suggested for many years, basically focusing on communications among devices in- and/or on-body, as well as between wearable devices, not exclusively phones, and external networks, like cellular ones or WiFi [3]. The list of applications for this type of networks has increased along the years, ranging from health to sports, encompassing military, police and civil protection ones, and reaching entertainment as well. There is already a wide body of knowledge in this area, although many aspects are still being researched (e.g., the impact of human mobility at the many several levels that need to be considered). Technology is already much developed in the area of wearable devices, and commercial offers already exist. Nevertheless, most of the work has been focused on the system and network aspects of this type of networks, not going much beyond on the issues that relate to

communication at external networks or at internal ones, like communication inside the human body.

Nano-networks are a more recent research topic, addressing communications inside the human body by devices that have dimensions of the scale of micro- and nano-meters, e.g., [4]–[6]. In this case, technology is still at an early stage and much of the research work is still at the theoretical level, although some prototyping can already be found [7], [8]. The common idea is to have devices inside the human body, at various levels, either implanted or mobile, e.g., in the cardiovascular or digestive systems. These devices can usually be considered either as bio-sensors, i.e., capable of sensing and collecting information on the human body, or as bio-actuators, i.e., releasing specific drugs to prevent or treat certain diseases. Of course, the information captured by bio-sensors needs to be transmitted to external networks, and bio-actuators need to be externally controlled as well. Thus, bio-sensors/actuators usually do not have a standalone approach, rather requiring communication with external networks, but this bridging has not been much addressed so far.

The applications of these networks in the medical area are many and varied. In particular, the disorders of the cardiovascular system are of high importance, as they are one of the main causes of deaths in developed countries, hence, their early diagnosis being very helpful to decrease the level of their fatal consequences.

Up to now, "networks" have been mentioned, but it is obvious that challenges do not occur only at the network level. Thus, the system level also requires much exploration, e.g.: frequencies bands, channel models, energy efficiency and impact of human behavior, just to name a few topics. In order to have a complete view of a nano-network application, we should address as well the way that communication is established between this network and the external one. BANs present themselves as a good relay option, since nano-nodes cannot communicate directly with external networks. A number of papers have already mentioned this global perspective, e.g., [9]–[13], but until now none has presented a global analysis from the network and system perspectives, which is the novelty of the current paper.

This paper deals with the problem of an artery occlusion, which is a fatally dangerous situation when the artery is blocked by a detached thrombus, i.e., a blood clot. The paper presents a new diagnostic system being able to detect artery occlusion, with suitable bio-sensors, and to prevent its consequences, with bio-actuators able to release appropriate medicines. Bio-sensors/actuators communicate with external devices via a bidirectional network composed of nano-nodes circulating in the cardiovascular system together with intra-body and body area components.

The paper is structured into 9 more sections, besides the current one. Section II presents the medical applications related to the human cardiovascular system. Section III shows the global network architecture, from the nano-nodes to the external networks, with the interfaces and frequency aspects. Then, Section IV addresses the nano-network model, more specifically the flow of the nano-nodes together with the communication system aspects, while Section V discusses the estimation of the number of nano-nodes required to detect a health problem and of the probability of activating a bio-actuator, both in an analytical perspective. System and communications aspects for the intra-body network are addressed in Section VI and for the body area network and the external one in Section VII. Finally, an analysis of the global system performance is done in Section VIII and conclusions are drawn in Section IX.

II. Medical Applications

Modern medicine relies on many diagnostic techniques for establishing patients diagnosis, monitoring diseases course and getting therapy results. The human body is an extremely complicated machine where various phenomena occur at the mechanical, biochemical or electrical levels, among others. As a consequence, there is plenty of methods to assess different functions of our organism, ranging from single molecules to cells and including organs (e.g., heart or liver) and whole systems (e.g., circulation or respiratory tract).

When we analyze the process of collecting information in different diagnostic procedures, in most cases it is a one-way process, where some parameters (e.g., concentration of certain molecules, temperature or images) are measured and sooner or later evaluated by a physician. However, there is a large group of disorders of the circulation and respiratory systems requiring a swift diagnosis and treatment in order to avoid serious irreversible damages or even death [14]–[16]. The first goal of diagnostic methods in these scenarios is to get the necessary information/parameters to identify the problem as soon as possible, followed by an immediate therapeutic intervention to restore the proper functioning of the damaged system. Thus, these situations would require two-way communications: out of the body for reporting the medical data gathered by diagnostic systems, and into the body for initiating therapeutic actions by medical staff.

An area that is especially fragile and prone to numerous dangerous situations is the human cardiovascular (i.e., the bloodstream) system, responsible for about 40% of human deaths in EU Member States [17]. One of the most common disorders is an artery occlusion, which means a decrease or total blockage of blood flow. The continuous and effective performance of the circulation

system is fundamental for all other organs functions, thus, an occlusion of blood vessels, especially arteries, leads to a decrease of blood supply, i.e., the oxygen and nutrients are not delivered to cells, followed by necrosis of ischemic tissues/organs. On the other hand, other disorders, such as bleeding (i.e., blood loss due to vessel damage), are also potentially critically dangerous and require immediate actions. In most cases, a suspicion of vessel occlusion is made indirectly and based on some typical symptoms or results from basic measurements, such as blood pressure or heart rate. Advanced laboratory or invasive techniques (PCI – Per-cutaneous Coronary Intervention) are applied to identify the precise location and to start a therapy, such as stent implantation or fibrinolysis, required to restore blood flow [14]–[16].

The most relevant situations when an artery occlusion requires a prompt reaction, to prevent serious irreversible damages, include brain stroke [14], myocardial infarction, i.e., heart attack [15], and Pulmonary Embolism (PE), a condition when a detached thrombus is flowing with blood and may block pulmonary arteries in some locations [16]. In all these cases a patient needs to be admitted to a hospital and optimal time to initiate therapy should not exceed 2 to 3 hours. Occlusion of arteries in pulmonary circulation requires a treatment different from arteries in systemic circulation, and also the treatment of a brain stroke is not the same as in the case of a myocardial infarction. Thus, immediate and precise information from inside the body about the location of an occluded artery would allow a proper planning of therapy schedule and drug selection. In some cases, communication into the body is crucial, e.g., in a severe PE affecting the hemodynamic efficiency of circulation or in a brain stroke, and proper drugs should be administrated within minutes, or up 1 to 2 hours maximum. In summary, two-way communications out of and into the body are required for early diagnosis, treatment planning and also for starting a therapy.

In this study, we focus on pulmonary blood circulation disorders. PE can be manifested in various scenarios, from irrelevant small artery occlusions, through the embolism with acute clinical symptoms and finally to the life threatening massive disorder requiring immediate actions [15], [18]. A typical reference test for the diagnosis of acute PE, considered as the most reliable one, is called Computed Tomographic Pulmonary Angiography (CTPA), where a contrast agent is injected into a pulmonary artery to identify the blocked vessels (the contrast is unable to fill occluded arteries) [19], [20]. This diagnostic procedure must be then interpreted by a radiologist. If CTPA is contraindicated or its results are inconclusive, a Ventilation Perfusion (V/Q) scan can be performed, which is based on inhaled and injected radioisotopes to visualise breathing (ventilation) and circulation (perfusion) processes in all areas of the lungs [21]. Historically, it was pulmonary angiography (PA) that was the gold standard for pulmonary embolism diagnosis (the contrast material is injected via a catheter introduced into the right part of the heart), however, nowadays PA is considered to be inferior to CTPA [22]. Finally, also Magnetic Resonance Angiography (MRA) was a promising diagnostic technique, but the results of large-scale studies do not recommend MRA as a first-line test due to its low sensitivity, low availability in most emergency settings and high percentage of inconclusive scans [23].

In practice, the average time between symptom onset and diagnosis of PE varies from 5 to 9 days [24]–[26]. Even after taking such a person to a hospital, the median time from admission to examination is about 3.5 hours [27] with main factors responsible for diagnosis delay being patients age, comorbidities and PE severity. A diagnosis time prolonged over 12 hours leads to increased mortality [27].

Considering all aforementioned factors, in this paper we propose a different approach where a person can be continuously monitored when she or he is leading a normal and active life. Our proposal is based on bio-sensors and bio-actuators installed in the pulmonary arteries and nano-nodes circulating in the bloodstream, Fig. 1. Monitoring by bio-sensors can reveal the narrowing of artery lumen before clinical symptoms appear. On the other hand, bio-actuators can release drugs locally in the region where the occlusion occurs, thus, allowing to avoid certain organs/tissues damage. Communication with an external network (and medical staff) is realized via the mobile nano-nodes and a body area network; the whole concept of a global network architecture is introduced in Section III.

It is worthwhile to stress that biotechnological capabilities, required for mounting bio-sensors/actuators into pulmonary arteries, already exist. Nowadays, the technology of intravenous interventions is well developed: there are various methods for the treatment of both arterial and vein issues, i.e., diagnostic angiography, angioplasty, atherectomy and stenting for arterial disease [14], [28], renovascular and mesenteric revascularizations for the former, and inferior vena cava filtration, deep venous thrombosis treatment, pulmonary emboli [15], varicoceles and varicose veins, venous occlusions (chronic and acute), and arteriovenous malformations for the latter. Thus, although the implantation of bio-devices in blood vessels can be easily achieved, an open issue is still the provision of reliable two-way communications between the numerous bio-devices and the medical staff, required for the effective monitoring of blood flow, the ability for timely diagnose artery occlusion and the start of treatment before any serious damages occur.

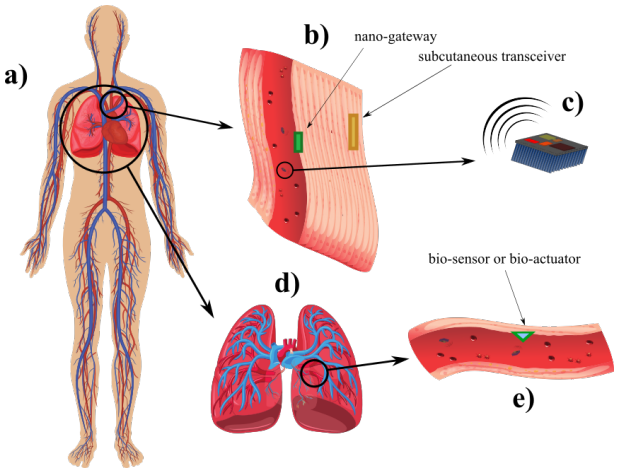

Fig. 1: General description of the nano-network for pulmonary embolism prevention: a) whole human vascular system; b) a superior vena cava (main vein) with a gateway node; c) an example of a mobile nano-node; d) pulmonary system of veins and arteries; e) an example of a pulmonary artery with a bio-sensor or a bio-actuator.

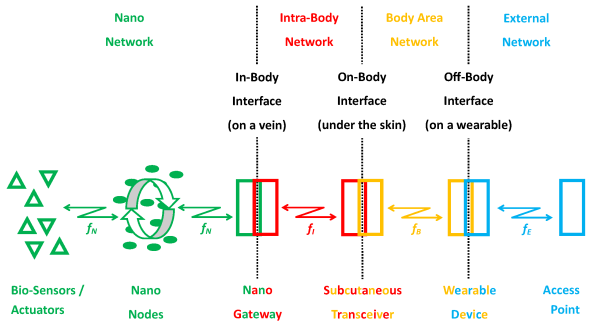

Fig. 2: Network architecture providing full communications between nano-devices and the external network.

III. Network Architecture

The proposed system is designed to perform three functions: (1) collecting information about a possible PE, (2) if appropriate, releasing medicines to dissolve thrombus and (3) providing two-way communications between the in-body devices and the medical staff, i.e., out of the patient's body and into it. The first two functions are realized with bio-sensors (collecting information) and bio-actuators (releasing medicine) located in pulmonary arteries. The two-way communications require a bidirectional system transporting the information from the cardiovascular system out of the body and vice-versa. It would be tempting to realize these communications directly between the bio-devices and a node located just under or on the skin, without any nano-network. It is, however, not feasible in practice for medical purposes: equipping all bio-devices with GHz interfaces would enlarge these devices to the size of centimeters, which is useless, having in mind the diameter of pulmonary arteries.

Fig. 2 shows a global view of the whole proposed system, with various sub-networks and corresponding interfaces. In what follows, we describe the components that are part of this system:

(a) *bio-sensors* are medical devices located in specific inner parts of the body, i.e., organs or tissues, measuring certain parameters. In the considered system, we assume that there are bio-sensors located in pulmonary arteries for detecting a possible embolism. Pulmonary arteries are part of the vascular system, which is very well known (e.g., [29]); it has one main artery divided into 3 smaller ones (2^{nd} level), which in total then divides into 8 branches (3^{rd} level), then into 20 branches (4^{th} level), and so on, until the 17^{th} level having about 3×10^8 branches. For the considered application, we suggest to have bio-sensors down to the 4^{th} level of the pulmonary system, at each of the 20 arteries, Fig. 1.d, since this level is a trade-off for the location of the bio-sensors: on the one hand, the blockage of the higher level arteries (1^{st}, 2^{nd} and 3^{rd}) can be detected at the 4^{th} level, and we just observe more than one 4^{th} level arteries blocked; on the other hand, lower level ($>4^{th}$) arteries are too thin to cause severe hemodynamic problems, so investigating all these single small arteries is not effective.
It is important to note that a bio-sensor located in the artery cannot measure the thrombus directly, as it can occur at any place of the artery. Instead, we propose that each bio-sensor constantly transmits a frame with its ID number, which can be received by nano-nodes flowing in the blood. When the blood flow is stopped by a thrombus in a specific artery, no nano-nodes receive frames with the respective ID, consequently, the thrombus can be detected by analyzing the statistical changes in the collected frames.

(b) *bio-actuators* are medical devices of another type: upon receiving a request, they are able of performing an action, e.g., to release medication such as alteplase, which causes the thrombus to dissolve [30], [31]. We assume that bio-actuators are placed at the first 3 levels of the pulmonary system at each of the 1+3+8 arteries, so, after a thrombus is detected by a bio-sensor, the alteplase can be released from a higher level artery.

(c) *nano-nodes* are relay nodes passing information from bio-sensors/actuators to the nano-gateway or vice-versa. Nano-nodes are circulating with the blood in the cardiovascular system [32] in a so-

called flow-guided nano-network [33]. They are of the size of about 8 to 10 μm and, because of their antenna size, they can communicate only in the THz band where range is limited to 1 to 2 mm [34]. These nodes have very restricted processing capabilities and a limited battery that can be periodically charged with a piezoelectric generator, thus, they can only transmit/receive at a certain time and only if the battery is loaded enough.

(d) a *nano-gateway* performs the function of a mediator between nano-nodes and the intra-body network. In the considered system, we propose to locate it on the wall of the superior vena cava, which is a large vein (diameter about 2 cm) in the human chest [35], well accessible for medical surgery operations and only 4 cm under the skin, Fig. 1.b. The nano-gateway has two wireless interfaces: a THz one to communicate with the nano-nodes and a GHz one with a larger range allowing for communication with the subcutaneous transceiver.

(e) a *subcutaneous transceiver* located just under the skin mediates between the intra-body and body area networks, enabling communications between the aforementioned nano-gateway and a wearable device. A single wireless interface is sufficient here, as both links, to the nano-gateway and to the wearable device, can be realized at the GHz band. This latter link, between the subcutaneous transceiver and the wearable device, should use a standard communications systems (e.g., Bluetooth or WiFi), so that a wide range of devices can be used, thus, providing a wide range of options for these devices.

(f) a *wearable device*, e.g., a smartwatch, a smartphone, a smart bracelet or another device enabling a connection to an external network. It also acts as a relay node, between the subcutaneous transceiver and the external network, with two wireless interfaces, the latter one being most probably based on WiFi or a cellular system.

The whole network operates in the following manner. Bio-sensors constantly transmit frames containing their ID, which are collected by mobile nano-nodes and later passed onto the nano-gateway. Frames are aggregated at the nano-gateway and transmitted to the subcutaneous transceiver, which forwards them to the wearable device, which in turn sends them to the external network. The medical staff can analyze the number of frames from all bio-sensors and check if their statistics are biased, i.e., if there are bio-sensors that do not deliver their frames, which can imply the blockage of the respective artery. Then, if the medical staff decides so, a request is sent to a specific bio-actuator to release a medicine dissolving the thrombus and unblocking the artery. The request is sent via a reverse link: via the wearable device, the subcutaneous transceiver, down to the nano-gateway, which broadcasts it to the nano-nodes. These nodes transmit it and eventually the frame is passed onto the proper bio-actuator.

This overall system is a complex mixture of technologies, at quite different stages of development. Basically, while higher frequencies and smaller scale nodes (i.e., THz bands and nano-networks) are still at an early research stage, the opposite lower frequencies and larger scale nodes (GHz frequencies for the intra-body and body area networks) are already offered commercially. Therefore, naturally, in what follows, attention is mostly paid to nano-networks, and then addressing the other sub-networks with a decreasing focus.

IV. Flow-Guided Nano-Network Model

The flow-guided nano-network model is derived from [33]. Nano-nodes circulate in the blood flow of the circulatory system, transmitting data to the nano-gateway that, in turn, sends data to the upper layers of the global network, up to the external network. The nano-device architecture used in this work is derived from [32], where a realistic nano-node model based on current technologies is presented. In this sense, the power and computational limitations of the nano-nodes translate into the following: i) they can only transmit one data frame per battery charging cycle and ii) they do not know the position of the gateway. The model has been extended and generalized to support our optimization problem.

A. Assumptions

The following assumptions are made (a summary of all variables used in this paper is given in the Annex.)

- There are N nano-nodes uniformly distributed along the flow, being in a closed circuit, i.e., continuously flowing in the vascular system. The total volume of the circuit is V_{net}.
- A nano-node requires, on average, a time $\overline{T_{cir}}$ to complete a round.
- The battery of a nano-node is charged at time intervals $T_{cha}(t)$,

$$T_{cha}(t) = \frac{1}{f_{cha}(t)} \tag{1}$$

where $f_{cha}(t)$ indicates that the recharging frequency can vary over time. Due to energy constraints [33], a nano-node can only transmit one data frame per battery charging cycle. Moreover, $f_{cha}(t)$ is bounded,

$$f_{min} \leq f_{cha}(t) \leq f_{max} \tag{2}$$

and the average charging frequency is $\overline{f_{cha}}$, e.g., the heart rate.

- Without loss of generality, let us assume that there are regions in the flow in which a nano-node is within the coverage zone of a nano-gateway, a bio-sensor or a bio-actuator of volume V_{cv}. A nano-node moves at an average speed v in the coverage zone, and since a nano-node cannot receive/transmit more than one frame when crossing this volume, the probability of a nano-node being in a coverage zone, p_{cv}, is modeled as:

$$p_{cv} = \frac{V_{cv}}{V_{net}} \tag{3}$$

- A nano-node does not know if it is within a coverage area, therefore, any nano-node attempts to transmit/receive a data frame during every battery charging cycle, which has two main consequences:
  1) Half of the energy is used in the transmitting mode and the other half in the receiving one.
  2) In order to minimize collisions, after battery charging all nano-nodes first listen to the channel for frame transmissions, nano-gateways or bio-sensors transmitting at this moment. Once channel listening is over, all nano-nodes attempt to transmit a frame, therefore, this avoids frame collisions between transmissions of bio-sensors and nano-nodes as they will transmit in different slots.
- A successful frame reception by a nano-node from a nano-gateway or a bio-sensor takes place if it starts and ends within its coverage volume. We define this region as the reception zone, with a volume V_{rx}, $V_{rx} < V_{cv}$, thus, the probability of a nano-node being in the reception zone is:

$$p_{rx} = \frac{V_{rx}}{V_{net}} < p_{cv} \tag{4}$$

- A successful frame transmission from a nano-node to a nano-gateway or a bio-actuator takes place if it starts and ends within the coverage volume and no frame collision occurs. We define this region as the transmission zone, with a volume V_{tx}, $V_{tx} < V_{cv}$, thus, the probability of a nano-node being in the transmission zone is:

$$p_{tx} = \frac{V_{tx}}{V_{net}} < p_{cv} \tag{5}$$

- A frame collision occurs if one or more transmissions start or end within the nano-gateway or bio-actuator coverage zone while another transmission in the transmission zone is taking place. Note that a node located outside the coverage zone can cause a collision if its transmission ends within this volume. We define the region in which a node may cause collisions as the collision zone of volume V_{cx}, $V_{cx} > V_{cv}$, thus, the probability of a nano-node being in the collision zone is:

$$p_{cx} = \frac{V_{cx}}{V_{net}} > p_{cv} \tag{6}$$

- We consider frames consisting of three fields: 1) *addressing* of length λ_h bytes, 2) other fields of length λ_o, and 3) *data payload* of length λ_d. Thus, frame size is

$$\lambda_f = \lambda_h + \lambda_o + \lambda_d \tag{7}$$

- The frame duration, t_f, depends on the frame size, λ_f and on the transmission bit rate, R; taking t_f as the time required to transmit a frame,

$$t_f = 8\lambda_f / R \tag{8}$$

then $t_f \leq T_{cha}(t)$.

B. Channel model

The channel model is based on the one described in [36]. Basically, the required transmission power for a frame, P_{tx}, depends on the gateway receiver sensitivity $P_{rx\ min}$, path loss coefficient α_{lin}, and distance d_{mm}:

$$P_{tx\ [\text{dBm}]} \geq P_{rx\ min\ [\text{dBm}]} + \alpha_{lin\ [\text{dB/m}]}\, d_{mm\ [\text{m}]} \tag{9}$$

where $P_{rx\ min}$ and α_{lin} are assumed to be constant, whereas d_{mm} can be configured according to the energy available in a nano-node battery.

Regarding the modulation to transmit data, we assume the well-accepted model for the transmission of femto-pulses, along with an on-off keying modulation [37]. This modulation assumes that energy is only consumed when transmitting bits with a logic value equal to 1, 0 being transmitted as silence, therefore, no energy is consumed in the transmission of the latter. The radio channel corresponds to a sequence of time windows during which a bit is transmitted using an electromagnetic pulse of a duration of $t_p = 100\,\text{fs}$. The duration between two consecutive bits is, in general, much longer than t_p.

For the sake of simplicity, we assume that the energy required to transmit or to receive a bit is similar. the one for a bit 1 symbol, $E_{b=1}$, being expressed as:

$$E_{b=1} = P_{tx}\, t_p, \tag{10}$$

whereas to transmit a bit 0 symbol, $E_{b=0} = 0$.

From (10), it is straightforward to derive that the maximum required energy to transmit/receive a frame, $E_{f\ max}$, corresponds to the case in which all bits in a frame of size λ_f are the bit 1 symbol. Moreover, if the amount of energy that a nano-node can store when it is fully charged is denoted as Q, and a nano-node can

receive/transmit a frame at every cycle, the following must hold:

$$E_{f\ max} = 8\,\lambda_f\,E_{b=1} \leq \frac{Q}{2} \tag{11}$$

The inequality in (11) shows that higher values of λ_f lead to lower values of $E_{b=1}$ and, consequently, to lower transmission powers and a smaller coverage area (following (9)).

Although it is out of the scope of this paper, we can assume that when a nano-node does not transmit, it acquires data or performs other tasks. In other words, a nano-node keeps consuming energy even if it is not transmitting. This power consumption is disregarded in our model, but it can be approximated by a fixed quantity of energy that can be added to Q.

C. Coverage zone model

In this paper, we follow a simple and intuitive model for the coverage zone, the main assumptions being summarized as follows:

- There is a spherical volume of radius d_{mm} (see (9)) around the gateway in which a transmission/reception can be successful if no frame collision occurs. All transmissions/receptions outside this region will fail. Frame collisions can happen when nano-nodes are transmitting to a nano-gateway or a bio-actuator, but not if it is the nano-gateway or the bio-sensor that is transmitting and nano-nodes are only listening.
- The antennas of the nano-gateway, bio-sensors, bio-actuators and nano-devices are isotropic.
- The coverage zone, V_{cv}, is defined by the intersection of a sphere of radius d_{mm} centered at the nano-gateway, the bio-sensor/actuator and a cylinder with a diameter equal to the respective vein or artery, D_{cyl}. The full derivation how to calculate this intersection for the known values of d_{mm} and D_{cyl} can be found in [38].

It is also necessary to consider the mobility of nodes in such flow guided nano-networks. To this end, it can be considered that a nano-node moves at an average speed $\overline{v}$ (it depends on the position of the nano-gateway or the bio-sensor/actuator) in the flow and that frame transmissions last t_f, the distance traveled by the nano-node, d_{nn}, being

$$d_{nn} = \overline{v}\,t_f \tag{12}$$

This derivation entails two new assumptions:

1) In order to successfully transmit/receive a frame, a transmission must start and end within the coverage volume, thus, if the node is close to leaving the coverage volume when the transmission/reception starts, then there is no time to finish it within this zone and the transmission fails. For this reason, an additional value of the successful transmission/reception zone, $V_{tx} = V_{rx}$, should be defined, which is smaller than the coverage zone, V_{cv}.
2) A collision occurs when two or more nano-nodes transmit within the coverage zone, thus, it is necessary to consider transmissions starting outside the coverage zone but ending inside it. For this reason, the volume corresponding to collision zone, V_{cx}, must be also considered.

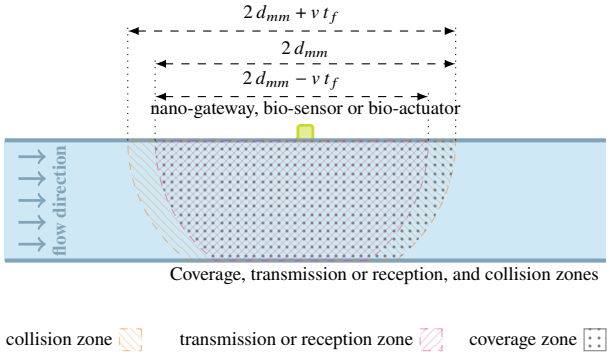

Fig. 3: Illustration of coverage, transmission/reception and collision zones.

The values of $V_{tx} = V_{rx}$ and V_{cx} can be calculated in a way similar to V_{cv}, having d_{mm}, D_{cyl}, $\overline{v}$ and t_f, by using the derivation from [38]. Fig. 3 illustrates the differences among coverage, transmission and collision zones (also for the equivalent model). Regarding the equivalent model, as nodes are uniformly distributed, it makes no difference to the analytical model.

To summarize, nano-node movement reduces the volume of the transmission zone, increasing the corresponding volume of the collision zone. Consequently, as it is not possible to set up the flow speed, a shorter t_f value (and shorter frame size, λ_f) improves the probability of successful transmissions. Moreover, in our model, the following condition must hold:

$$d_{nn} < 2\,d_{mm} \tag{13}$$

This condition guarantees that any arbitrary node crossing near the nano-gateway or the bio-actuator will have the chance to successfully transmit/receive a frame. Note that, for negligible values of d_{nn}, there are no transmission range requirements, although higher values of d_{mm} lead to higher coverage, transmission/reception and collision volumes. For non negligible values of d_{nn}, inequality (13) guarantees that volume $V_{tx} = V_{rx}$ is large enough to allow complete frame transmissions ($V_{tx} = V_{rx} > 0$).

An example of transmissions/receptions and collisions can be found in Fig. 4. For a successful transmission, a

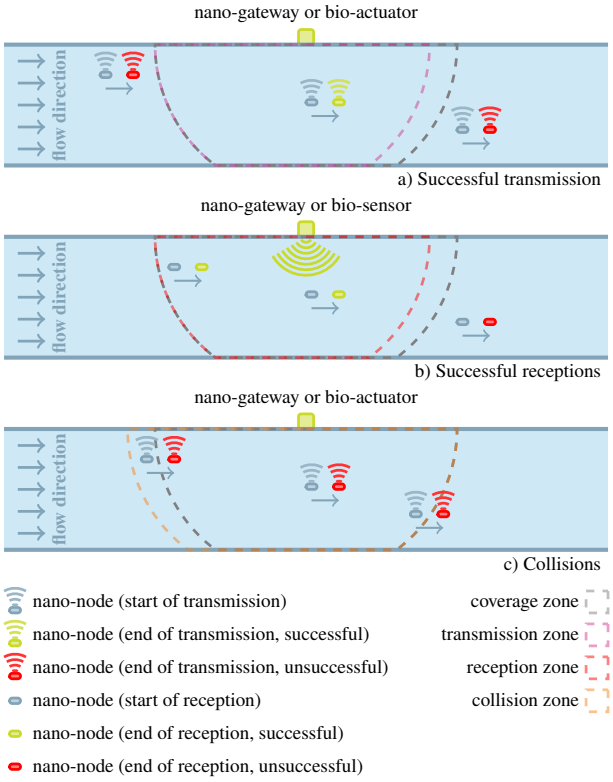

Fig. 4: Illustration of successful transmissions and receptions, and collisions.

nano-node must be alone within the transmission zone when it starts sending a frame; note that only one successful transmission is possible at the same time. Similarly, a successful reception happens if a nano-node is within the reception zone when the transmission starts; in this case, more than one successful reception is possible in the reception zone as no collisions can happen. Collisions can happen if two or more nano-nodes start or end a transmission within the coverage zone.

D. Frame structure and duration

There are some proposals in the literature dealing with MAC protocols for nano-networks [39]–[41], but none consider the particularities of flow-guided nano-networks. It is outside the scope of this paper to provide a detailed frame structure (which depends on the particular protocol implementation), however, it is important to differentiate between the size of the frame data payload and the remaining fields, thus, we propose a very simple frame structure that is used in our optimization problem:

- Addressing field of size λ_h: we assume that a frame contains at least two addresses (for sender and receiver, respectively), hence, if the nano-network contains N nano-nodes plus a gateway, then the following must hold:

$$\lambda_h \geq 2 \left\lceil \frac{\log_2 (N+1)}{8} \right\rceil \tag{14}$$

- Other fields of constant size λ_o: within this category checksums, frame size, etc., can be included.
- Data payload of size λ_d: its size is determined by medical application requirements.

From this basic frame structure, we derive the total frame size, (7). Regarding the time required to transmit a frame, t_f, when the nano-node transmits at a bitrate R, it is defined by (8). Moreover, t_f is subject to the constraint $V_{tx} = V_{rx} > 0$, i.e., as longer values of t_f reduce $V_{tx} = V_{rx}$, there is a limit for t_f, otherwise, no transmissions are possible.

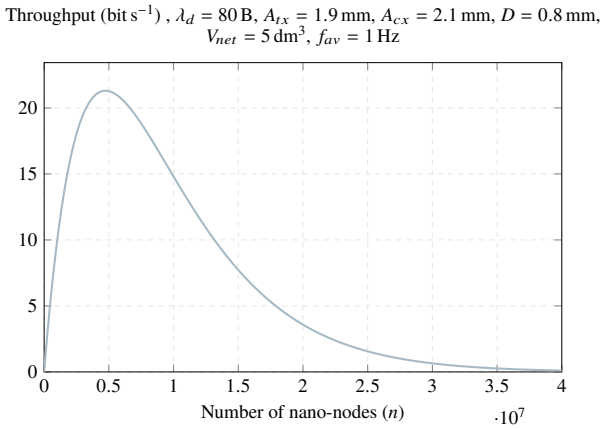

Fig. 5: Illustration of the relationship between the number of nano-nodes and achieved throughput.

E. Nano-node transmission model

The throughput of a flow-guided nano-network, θ, has already been presented in [33] in frame/s, being reformulated in bit/s as:

$$\theta = \frac{8\,\lambda_d\,N\,\overline{f_{cha}}\,V_{tx}}{V_{net}} \left(1 - \frac{V_{cx}}{V_{net}}\right)^{N-1} \tag{15}$$

Expression (15) represents the amount of data that can reach the nano-gateway, beign related to the probability of a nano-node performing a complete transmission within the coverage volume when no collision occurs. Fig. 5 shows that throughput increases as the number of nano-nodes grows to a certain value, beyond which increasing the number of nano-nodes throughput decreases, since the probability of collisions starts to be significant (there are too many nano-nodes in the flow-guided nano-network).

Additionally, the work in [33] shows interesting facts about these flow-guided nano-networks:

1) There is a value of the number of nano-nodes, N_θ, that maximizes throughput for any network setup, which is derived from (15) [33]:

$$N_\theta \approx \frac{V_{net}}{V_{cx}} \tag{16}$$

2) The size of the coverage volume is not relevant to achieve a larger throughput, however, following (16), a higher value of V_{tx} and V_{cx} requires fewer nano-nodes to achieve maximum throughput.

Note that the time required for a nano-node to complete a round in the flow-guided nano-network,T_{cir}, is not significant in terms of throughput, the relevant parameters being V_{net}, V_{tx}, V_{cx}, and N (V_{tx} and V_{cx} can be generally approximated by V_{cv} for negligible values of d_{nn}).

V. Estimation of implementation parameters

The goal of the following analytical estimation is to obtain a minimum threshold of the number of nano-nodes that guarantees with a given probability (p_{Qd}) that no false detection is performed. To this end, we can start by calculating the average number of successful frames received by the nano-nodes during a round:

$$\overline{r_T} = N\,\overline{f_{cha}}\,\overline{T_{cir}}\left(\frac{V_{rx}}{V_{net}}\right) \tag{17}$$

thus, as a nano-node uniform distribution is assumed and a nano-node cannot receive more than one frame per round, the probability that a nano-node receives a frame is:

$$p_{rx,T} = \frac{\overline{r_T}}{N} = \frac{\overline{f_{cha}}\,\overline{T_{cir}}\,V_{rx}}{V_{net}} \tag{18}$$

After τ time slots, the probability of a nano-node having received at least a frame from a bio-sensor can be modeled as:

$$p_{rx,T,\tau} = 1 - (1 - p_{rx,T})^{\tau/\left(\overline{f_{cha}}\,\overline{T_{cir}}\right)} \tag{19}$$

The system fails if the artery in which the bio-sensor is placed is not blocked and no frame transmitted from it arrives to the gateway, thus, for every time slot, a failure happens if the gateway receives a frame not containing any information from the bio-sensor or does not receive anything, equivalently, being the probability of not receiving a successful notification from the bio-sensor, p_f, which can modeled by:

$$p_f = 1 - \frac{N\,V_{tx}}{V_{net}}\left(1 - \frac{V_{cx}}{V_{net}}\right)^{N-1} p_{rx,T,\tau} \tag{20}$$

The probability that after τ time slots no bio-sensor detection happens is:

$$p_{f,\tau} = (p_f)^\tau \tag{21}$$

As the final goal is to dimension the network to obtain a $p_{f,\tau}$ bellow a given threshold, i.e., $1 - p_{Qd}$, the following must hold:

$$p_{f,\tau} \leq 1 - p_{Qd} \tag{22}$$

If $1 - p_{Qd} \to 0$, (22) can be approximated by:

$$\frac{\tau\,N\,V_{tx}}{V_{net}}\left(1 - \frac{V_{cx}}{V_{net}}\right)^{N-1} p_{rx,T,\tau} \geq p_{Qd} \tag{23}$$

Beyond the detection of a blocked artery, it is also important to estimate the probability of receiving a frame if the artery is non-blocked. In this sense, τ can be interpreted as the time in which the nano-node remembers it has received a message from a bio-sensor. In other words, a nano-node remembers a frame reception from a bio-sensor during τ time slots. Thus, let us define ϵ as the elapsed time slots since the last bio-sensor detection, and $p_{d,\tau,\epsilon}$ as the probability of receiving a frame before ϵ time units if a nano-node remembers a bio-sensor frame reception for τ time units. From (21) it is straightforward to derive $p_{d,\tau,\epsilon}$ as:

$$p_{d,\tau,\epsilon} = 1 - (p_f)^\epsilon \tag{24}$$

Expression (24) converges to 1 as ϵ increases, this convergence being faster for higher values of τ. This is consistent with the fact that higher values of τ increase the probability of more nano-nodes in the system with received frames from the targeted bio-sensor.

Finally, it remains to obtain the estimation of the probability for activating a bio-actuator. Once a bio-actuator has to be activated as a consequence of a medical issue, it is important that this activation can happen within a given deadline with high probability. To this end, we assume that nano-nodes receive the order of activating a given bio-actuator from the nano-gateway, and that, at the beginning, no nano-node has received an activation order.

Thus, similarly to (19), the probability that a nano-node receives an activation order in M rounds can be obtained as:

$$p_{rx,T,M} = 1 - (1 - p_{rx,T})^M \tag{25}$$

from which it is possible to calculate the probability of successfully performing an activation of a bio-actuator in round M, $p_{a,M}$, as:

$$p_{a,M} = 1 - \left(1 - \frac{N\,V_{tx}}{V_{net}}\left(1 - \frac{V_{cx}}{V_{net}}\right)^{N-1} p_{rx,T,M}\right)^{\overline{f_{cha}}\,\overline{T_{cir}}} \tag{26}$$

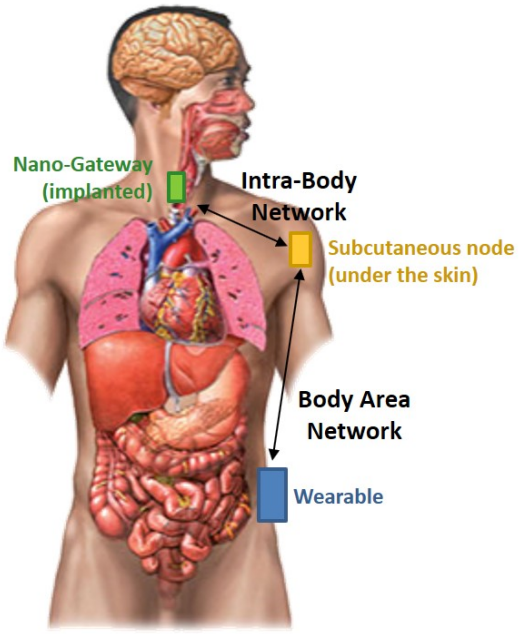

Fig. 6: Intra-Body and Body-Area Networks.

The final goal is to dimension the network so that a bio-actuator gets activated in less than ϕ rounds with a very high probability, p_{Qa}:

$$\prod_{k=1}^{\phi} (1 - p_{a,k}) \leq 1 - p_{Qa} \tag{27}$$

Having established the model for the nano-network, the other subnetworks need to be characterized as well.

VI. Intra-Body Network

Once the information carried by nano-nodes is collected by the nano-gateway, its delivery towards a device outside of the body is another important challenge. As aforementioned, we propose an intra-body link between the nano-gateway and a subcutaneous implant using radio frequency techniques in order to overcome the gap between the circulatory system at the nano level and the outer level of the body, this approach being illustrated in Fig. 6.

Intra-body (also called in-body or implanted) radio communications have been widely addressed in the literature. Until today, the Medical Implant Communications Service (MICS) band at [402, 405] MHz has been used by medical devices for data transmission, due to the low losses of body tissues at these frequencies. However, its offered low data rates and especially the antennas large size at these frequencies lead to the exploration of higher frequency bands [42], [43].

Recently, Ultra-Wide Band (UWB) technology has been proposed for the operation of ingestible devices due to its large bandwidth, [3.1, 10.6] GHz, high data rates, low power consumption and miniaturization capabilities [44]. However, human body tissues exhibit a large attenuation at UWB frequencies and this attenuation is frequency dependent. Thus, the lower part of the UWB band [3.1, 5.1] GHz has been recommended for wideband in-body communications [45], [46], especially for a Wireless Capsule Endoscopy (WCE) scenario where high-quality video transmission is required.

The Industrial, Scientific and Medical (ISM) band, [2.4, 2.5] GHz, has been also proposed for the operation of in-body devices. Despite the lower offered data rates compared to UWB, it can provide a good trade-off among miniaturization capability, path loss and occupied bandwidth, thus, being an ideal technology to transmit data from inside the human body in case of moderate data rates. More specifically, the ISM band has been recently proposed to be used in the future generation of leadless pacemakers, where an in-body antenna will be implanted inside the heart and a subcutaneous antenna is configured as receiver. It was found that the ISM band is optimal for this kind of communications, due to the combination of the inherent path loss of the biological tissues at these frequencies and the high achievable efficiency of the antenna [43].

In the last years, several works have analyzed communications in this area, using the 2.4 GHz band for cardiac applications. Concretely, in [43] the authors analyse implant to subcutaneous communications, for three different positions of the subcutaneous receiver. It was found that the path loss (also called coupling in other studies) was optimal (minimum) when installed subcutaneously in the outer wall of the abdomen. Nevertheless, this position can cause discomfort to the patient in a real application, which the authors propose to solve with a multi-nodal solution. The same issue was found when locating the receiver in the lateral side of the body, in addition to the larger path loss found for this configuration. Finally, the shoulder was also explored as a potential location for the subcutaneous receiver, due to its easy access and comfort for the patient, but this arrangement leads to an increment of 13 dB in path loss.

Antennas also pay a key role in link evaluation. Antennas performance not only depends on their own design, but also of the surrounding tissues where they operate [47]. This is particularly important for implanted antennas at GHz frequencies, where surrounding organs commonly are high-water content tissues with large permittivity, thus, being extremely important to design and optimize antennas considering all tissue layers present between the implanted transmitter and the subcutaneous receiver [48].

Several candidates for both implanted and subcutaneous antennas that have been proposed in literature for the cardiac scenario so far. In [43], [49], a planar meander antenna with $11.96 \times 5 \times 3.5$ mm^3 is conformed inside a capsule to be implanted inside the heart, while a rigid planar antenna of 30×30 mm^2 is proposed for subcutaneous operation; however, both antenna designs are not flexible enough for a real application over the surface of the vena cava. The same problem was found in the dual-band antenna proposed in [50]. In [51], the authors present a flexible antenna with $7 \times 7 \times 2$ mm^3, but this antenna was designed to operate in the scalp, which is a much less delicate area compared to the superior vena cava. A similar situation was found in [52], where the proposed antenna is optimized to work at 2.4 GHz and 4.8 GHz, exhibiting a really reduced size (7.7×6.9 mm^2), but it is neither flexible nor designed to operate deeply implanted. As mentioned before, the final performance of the in-body link has to be taken into account, which is influenced by the definite antenna design.

Considering the scenario of this work, where the gateway is attached to the superior vena cava, the arrangement of both in-body and subcutaneous antennas is very similar to the one proposed in literature for leadless pacemakers. In this scenario, the signal needs to be transmitted from the external wall of the superior vena cava (with a depth of 4 cm) to a remote receiver, which implies data transmission throughout the thorax; besides, the antenna's surrounding tissues are nearly the same as in the cardiac scenario (blood, veins, muscle and subcutaneous fat). Therefore, the ISM 2.4 GHz is the most suitable band to transmit data gathered from the nano-network, due to the affordable path losses at these frequencies along with their offered moderate data rates. Besides, the implanted and subcutaneous antenna models already outlined for cardiac applications can be used as a starting point for the design of antennas for the intra-body link. The main difference here is that the in-body antenna should be really ultra flexible and tiny, in order to be implanted inside the human body, and particularly over the surface of the vena cava. Current research on biocompatible and flexible materials shows promising achievements in the near future in this field [53]–[55]. Similar requirements are needed for the subcutaneous implant, although its features are not so restrictive in terms of flexibility and size.

VII. Body Area and External Networks

Having delivered the sensory information from the nano-network to the subcutaneous node, the remaining task is to further transport data to a nearby wearable device or communication infrastructure, Fig. 6. Still, in order to do so, given that the subcutaneous transceiver is a very low power device, the approach taken is that this transceiver establishes an on-body communication to a wearable device (e.g., a smartphone or a smartwatch), and then this device enables the off-body communication to the external network (via a cellular system or WiFi). Nevertheless, a discussion on this matter is in order.

With the transceiver placed under the skin, to minimize tissue penetration losses, communication to the external network can be realized in two ways. In one approach, we can assume that the transceiver is capable enough to establish a connection directly to the external network, but this seems a reasonable choice only if this link is established over short distances, such as in specific indoor environments, e.g., hospital rooms. In another approach, we can seek for a wider range of applications, where the constraints on small size, low-energy and comfort typically limit the complexity of these transceivers; in this case, the link should use a wearable device as a relay, which allows for a longer off-body communication range and access to several communication technologies typically available in such devices, however, at the expense of an additional on-body communication link introduced to the data delivery chain.

On-body communications from subcutaneous devices has already gained the attention of researchers and the literature has a number of works in this area. The key problem, from the communications system viewpoint, is to characterize the channel, namely path loss, so that one can estimate a proper link budget for the link. The authors in [56] present a model for the estimation of system loss, for varying thicknesses of skin, subcutaneous fat, abdominal muscle and visceral fat, overall roughly between 20 mm and 150 mm, at both 403 MHz and 923 MHz, with average values ranging in [4.4, 15.5] dB for the former and [6.8, 15.1] dB for the latter frequencies. Measurement results for path loss are presented in [57] and a fitting model, for a frequency centred at 1.85 GHz, for distances between 17 cm and 40 cm is proposed, the average path loss varying between roughly 47 dB and 59 dB, when the subcutaneous antenna is placed 11.5 cm under the skin. The authors in [58] present the design of an external matched horn antenna for subcutaneous links, working at the 2.4 GHz ISM band, with transmission losses ranging between roughly 8 dB and 39 dB for depths under the skin between 4 mm and 50 mm, while [59] presents a novel antenna for pacemakers, where the subcutaneous placed antenna is powered via an external source, operating at 924 MHz with a quite acceptable overall efficiency of 65%. Also, [60] addresses a subcutaneous novel antenna design for the 1.4 GHz Wireless Medical Telemetry Service and 2.4 GHz ISM bands; experiments (on pigs) successfully

show the transmission of data through the tissue and skin, with system losses ranging between roughly 60 dB and 90 dB for depths under the skin between 1 mm and 20 mm.

Of course, path loss depends on the location of the subcutaneous transceiver as well as on the one for the wearable device. Its average value can be smaller, and with a low variability, for a transceiver in the chest and a wearable device on the belt, while it can be larger, and with a high variability, for the same transceiver location but with the device being a smartphone or a smartwatch (which have a much larger mobility, hence, signal variability). Constraints imposed by the transceiver's antenna and transmit power will define the precise link budget limitations.

With a number of mature radio communication technologies being available for employment in this link, most notably Bluetooth, Bluetooth Low Energy, ZigBee and UWB being among the technologies acknowledged by IEEE 802.15.6 [61], we can expect that this link will tend not to use a brand new technology, but rather a version of these ones, with the proper modifications (e.g., to account for power limitations and to minimize interference). Moreover, in order to simplify the design of the subcutaneous transceiver, and to accommodate the low size and low power requirements, we envisage that the same system is used for the links with both the nano-gateway and the wearable device, in a time-shared mode (i.e., time division duplexing - TDD); since the required data rates are not that high, the TDD mode can be easily implemented in the transceiver.

In both on- and off-body communication links, several important challenges exist, [62], namely body-shadowing and depolarization losses, with an important impact of user dynamics, yielding a non-stationary channel [63]. By considering that an outage event in one of these links can mean a loss of sensitive information whose delivery from the source to the external node requires a considerable effort by the nano-nodes, this segment of the system is an important link in the chain, and its reliability plays a notable role in the overall system performance.

Body-shadowing occurs when the user (in on- and off-body links) or another person (in off-body links) obstructs the Line-of-Sight (LoS) propagation path, thereby introducing excess losses up to 30 dB [64], [65]. The low elevation and proximity of wearable antennas to the body make this effect particularly challenging in BAN communications, where a simple user rotation brings the antenna deep into the shadowed region [66].

The main difference in body shadowing characteristics among on-body antenna locations essentially comes from the different motion dynamics. Most notably, the wearable antennas on the arms and legs, e.g. a smartwatch, benefit from the swinging motion that takes them in and out of the shadow region, thereby yielding a reduced overall impact of body shadowing. With blockage periods being predictable for typically cyclic human motion, e.g., walking and running, appropriate scheduling algorithms exploiting the knowledge from motion sensors can be employed to maximize transmission efficiency [67].

The severity of body-shadowing also varies among different scenarios. For example, losses are expected to be lower with the user walking around a room, compared to the case when the user is lying on a bed. While the diversity stemming from the existence of several propagation paths in different directions dampens the impact of individual path shadowing on the total receiver power in the former case, in the latter one the wearable antenna can find itself completely covered between the user and the bed. Communication outages in such cases can be avoided by means of spatial diversity, with a pair of antennas employed at different sides of the body [68]. However, the improved robustness of the system comes at the expense of the inconvenience associated with wearing several devices instead of one, an option likely acceptable by users only in critical scenarios, i.e., emergency room monitoring.

Signal depolarization is another important effect [69], with polarization mismatch losses arising due to signal depolarization in the propagation environment [70], [71], antenna depolarization in the proximity of the lossy body tissue [72], and to the wearable antenna rotation during motion [63]. The polarization of wearable patch antennas is reported to change from a linear one in free space to an elliptical one when placed near the body, with a shorter distance from the body yielding a higher degree of depolarization. For example, the polarization of the antenna considered in [69] is vertical with the Cross-Polarization Isolation (XPI) being above 10 dB over 99% of the radiation sphere in free space. However, this percentage is only 30% for the antenna at 2 mm from the body.

The dynamic rotation of antennas on arms and legs during motion results in high and variable polarization mismatch losses, compared to the nearly static antenna placements on the torso or the head. For a simple simulated scenario with the user running in [69], these losses are below 1.5 dB for the antenna on the torso, while reaching -42 dB and -34 dB for wrist and lower leg placements, respectively. Considering that the depolarization effect can yield a complete loss of energy transmission over the LoS path without its being physically obstructed, it has an important influence on the link outage and system performance. To mitigate these effects, polarization diversity with co-located cross-polarized antennas offers a convenient solutions [73]–[75], at the expense

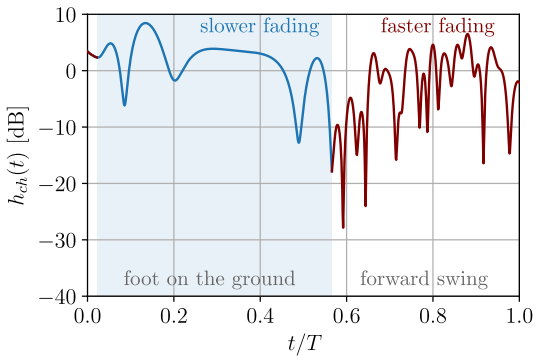

Fig. 7: Multipath fading realization during a walking cycle for antenna on the lower leg.

of a somewhat more complex receiver structure.

The wearable antenna motion also affects signal fading characteristics. While fading dynamics are essentially time-invariant for static antenna placements on the chest or the head, the periodic displacement of antennas on arms and legs yield non-stationary fading. For these dynamic locations, two distinct phases with slow and fast fading dynamics phases are observed during walking/running cycles [76], e.g., during the backward and forward swings of the arm/leg, respectively. The fast phase is characterized by more than 4 times faster signal variation for dynamic antenna placements on arms and legs, while the slow one yields longer average fade duration. This is illustrated in Fig. 7, showing a fading realization during one walking cycle for an antenna on the lower leg. With the two phases being predictable, link adaptation and scheduling algorithms as [67] can be used to maximize transmission efficiency.

VIII. System Performance Analysis

Having discussed the network architecture and its nano, intra-body and body-area networks, in this section we analyze the performance of the whole system. We assume a viewpoint of medical doctors who deal with pulmonary circulation disorders and would like to use the system to detect an artery occlusion, i.e., a situation when an artery is blocked for blood flow. We assume $N = 20$ bio-sensors located in pulmonary arteries and continuously transmitting beacon signals with their ID. Nano-nodes, flowing nearby, wirelessly collect frames from bio-sensors and forward them to the gateway node, the frames being further sent to the subcutaneous node and eventually reach the wearable device (e.g., a smartphone). Finally a medical doctor can check the data and if no frame comes from a specific bio-sensor, an artery occlusion can be suspected, and the doctor can initiate the second stage of system activity, by sending a request to a bio-actuator in a pulmonary artery to release medicines helping to remove the occlusion and restore the correct blood flow. The request frame should travel a similar way back through the whole system: from the wearable device to the subcutaneous node, then to the nano-gateway and finally via nano-nodes to the chosen bio-actuator.

Having this in mind, the system performance analysis is focused on studying how quickly the system can react depending on the concentration of the nano-nodes in the blood. We calculate the reaction times in both stages of the system operation: (a) how quickly the doctor can get the information about the occlusion after it happens and (b) how quickly a bio-actuator can be triggered after the doctor sends a request.

The parameters for the analysis are shown in Table I. The concentration of the nano-nodes in the blood varies from 10 to 200 per cm^3, the other parameters being based on earlier studies in this topic, assuming communication in the THz band with the transmission rate of $1\,\mathrm{Mbit\,s^{-1}}$ [38]. Taking the propagation environment into account, which is blood, the communication range is assumed to be approximately $1\,\mathrm{mm}$ [36], the size of the frame is $64\,\mathrm{B}$ and the charging frequency is $1\,\mathrm{Hz}$ [77]. For the intra- and off-body system parts, which both work at the 2.4 GHz band, the transmission power, receiving sensitivity and the throughput are also given in Table I.

As results demonstrate, the bottleneck of the whole system lies in its nano-network part, which is expected considering the very limited communication range of nano-nodes (in the order of millimeters) comparing with the length and volume of the human bloodstream, thus, the analysis is about the nano-network mainly. For the intra- and body-area parts, we focus on link budgets proving that the system is working reliably and with delay orders of magnitude lower than those for the nano-network.

A. Nano-network

Both stages of system activity are analyzed. First, the scenario of gathering data frames from bio-sensors is considered in Fig. 8: given the concentration of nano-nodes in the blood and the elapsed time, we calculate the probability p_Q that the nano-network delivers a frame from a specific bio-sensor in the elapsed time t. The frames are also kept no longer that t minutes in the nano-nodes memory, so p_Q can be interpreted as the probability of detection of the artery occlusion (if it happened) in the last $2t$ minutes. Taking a concentration of 100 nano-nodes per cm^3 in 1 h the probability is around 45% increasing to 78% in 2 h, while for double concentration, we get around 60% and 97%, respectively; these results show that in a time interval

TABLE I: System parameters used for the analysis.

Parameter	Value
Nano-network:	
Nano-nodes concentration	10-200 per cm^3
Frequency band	0.1-10 THz
Transmission rate	1 $Mbit\,s^{-1}$
Max. Tx power	1 mW
Pulse duration	10^{-13} s
Path loss	130 dB/mm
Rx sensitivity	-130 dBm
Frame size	64 B
Charging frequency	1 Hz
Battery energy	19.2 fJ
Total blood volume	4.8 dm^3
Blood velocity	13-16 $cm\,s^{-1}$
Intra-body network:	
Frequency band	2.4 GHz
Transmission power	-24 dBm
Receiver sensitivity	-90 dBm
Throughput	4.8 kbit/s
Body area network:	
Frequency band	2.4 GHz
Transmission power	-5 dBm
Receiver sensitivity	-82 dBm
Throughput	125 kbit/s

between 1 h and 2 h, reasonable results are obtained, 3 h being enough for an operation of the system with a very high probability for medical purposes.

Another view on system performance is presented in Fig. 9, where the probability of receiving a frame from a specific bio-sensor is given assuming that nano-nodes keep frames in memory by τ minutes. Taking again 1 h and 2 h, we get a probability around 63% and 87% for 1 h memory and 87% and 97% for 2 h, respectively, reinforcing the idea that the time interval between 1 and 2 h seems to be enable a good choice for system performance, 3 h leading once more to a very high probability. This is a view that a medical doctor or the patient himself could have: the frames from each bio-sensor should be observed in time T with the given probability. If the probability is very high and no frames are observed, it is a clear indication that an occlusion is highly probable and an alarm should be triggered.

The second stage of system activity is related to the scenario when a medical doctor would like to activate a bio-actuator, e.g., after discovering the artery blockage. The results in Fig. 10 present the probability of activation of a chosen bio-actuator in the elapsed time of t minutes. As this probability depends of the average nano-node concentration and the bio-actuator coverage zone volume, it is the same for bio-actuators at 1st, 2nd and 3rd levels. Taking again a concentration of 100 nano-nodes per cm^3 in 1 h the probability is around 25% increasing to 50% in 2 h, while for double concentration, we get around 37% and 73%, respectively; we can conclude that if the whole system is designed to enable

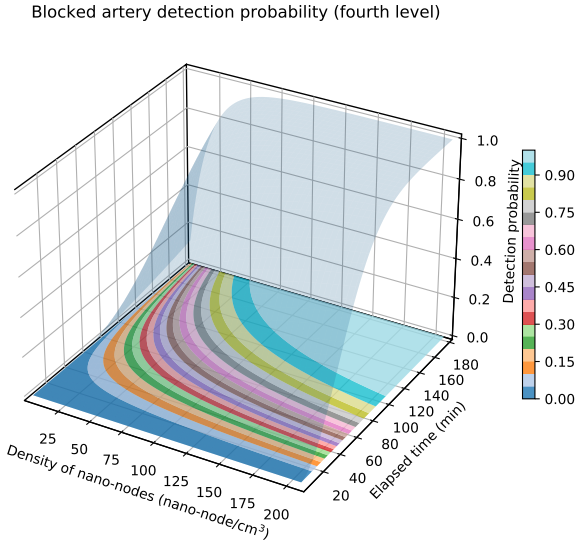

Fig. 8: Probability of frame delivery from a bio-sensor via the nano-network.

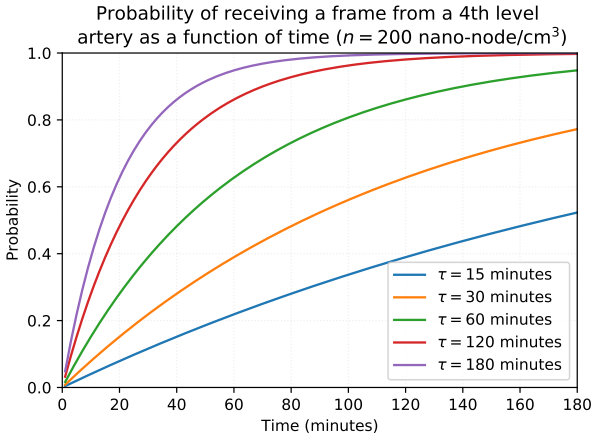

Fig. 9: Probability of receiving a frame from a bio-sensor as a function of time, 200 nano-nodes per cm^3.

a medical reaction for an occlusion in a few hours, the concentration of nano-nodes in the blood should be at least 150 per cm^3.

B. Intra-body network

In the case of the intra-body link between the nano-gateway (implantation depth of around 4 cm) and the subcutaneous node, a preliminary analysis can be performed by means of phantom-based measurements. To achieve this goal, two different setups were configured and are depicted in Fig. 11: a) heart muscle phantom (1-layer configuration); b) heart muscle and fat phantoms (2-layer configuration). It should be noted that although experiments in [78] were designed for heart tissue, blood

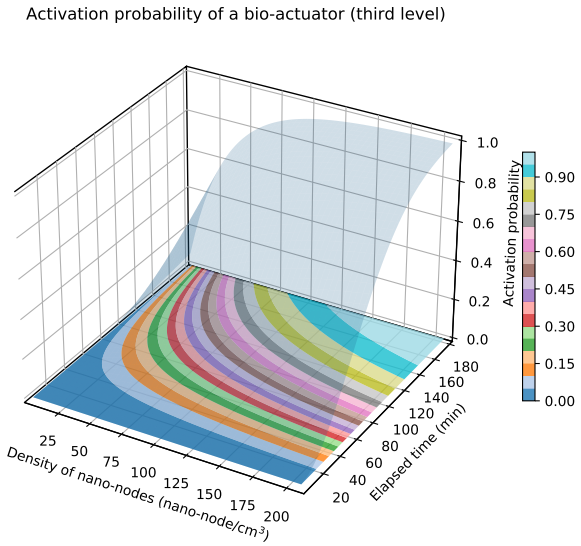

Fig. 10: Probability of activating a bio-actuator.

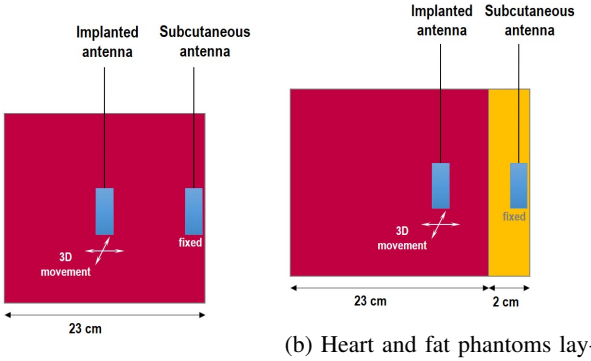

(a) Heart phantom layer.

(b) Heart and fat phantoms layers.

Fig. 11: Phantom-based measurement setup.

and heart have nearly the same dielectric properties, so that the subsequent liquid phantom formulation is nearly identical. For both configurations, phantoms were poured into a squared plastic container whose size is $25 \times 25 \times 25$ cm^3 in order to replicate the human chest.

The transmitting antenna was immersed into a liquid phantom that aims to replicate the dielectric properties of the heart/blood. The receiving antenna was located on the inner wall of either the heart phantom layer, Fig. 11a, or the fat phantom layer, Fig. 11b, thus, the subcutaneous receiver was emulated.

The implantable antenna was a conformable meander antenna [43], whose location was controlled automatically by using a 3D cartesian positioner. On the contrary, the subcutaneous antenna [43] was fixed at the internal wall of the phantom container and it was designed as a rigid patch antenna. More details about these experiments can be found in [78], [79].

Considering the two configurations aforementioned, it was found that the path loss was well fitted by the typical log-distance model:

$$L_{p\ [\mathrm{dB}]} = L_{0\ [\mathrm{dB}]} + 10\,\alpha_{log}\log(d/d_0) + N(0, \sigma_{[\mathrm{dB}]}) \quad (28)$$

where L_0 is the path loss at the reference distance d_0, which is taken as 4 cm, α_{log} is the average power decay, and $N(0, \sigma)$ is the Normal Distribution, with zero mean and standard deviation σ. Models are almost identical regardless of considering fat or not, as it can be seen in Table II, which is due to the fact that the fat layer only adds extra loss but does not modify the trend of loss with distance [80]. For both cases, path loss for a distance of 4 cm between the implanted transmitter and the subcutaneous receiver is around 22 dB, which means that communications in 2.4 GHz between the superior vena cava and the surface of the body would be easily feasible. For the sake of comparison, if the UWB band was considered, the link loss for 4 cm is more than twice than the one for ISM (54.2 dB). This would lead to a more complex scenario where much higher losses should be compensated for, managing a successful communication between the nano-gateway and the exterior of the body.

TABLE II: Path loss models in the chest area for ISM band from phantom measurements.

	Heart muscle	**Heart muscle + fat**
L_0[dB]	22.92	21.85
α_{log}	4.12	4.12
σ[dB]	7.3	4.5

Regarding link performance, an output power of -24 dBm [81], regardless of the modulation scheme, is enough to achieve an acceptable bit error rate in these kinds of devices. On the other hand, during experiments, the receiver's sensitivity was measured to be -90 dBm [78]. Considering 22 dB to 23 dB of path loss for 1- or 2-layer configurations, respectively, the link budget reveals a really feasible communication for the intra-body link. The throughput for this link is 4.8 kbit/s, as it can be also obtained from [81] where the same equipment is used. Considering the data coming from the nano-network, the gateway should be able to send packets containing a number of frames coming from each bio-sensor (an integer number, 32 bits) for 20 bio-sensors, once per second, which is only 640 bit/s. We can then conclude that the available throughput is more than the one required for this medical application.

C. Body area and external networks

As mentioned before, the off-body connection between the wearable device and the external network can

be easily implemented via WiFi or a cellular system, hence, being well-known and easily characterised, without imposing any limitations to the overall system.

Assuming that the on-body connection is implemented in Bluetooth LE, the data rate is more than enough to satisfy the application requirements, even if just half of its maximum is taken due to the TDD mode. The power difference (between transmitter and receiver) is 77 dB (Table I), which seems to be enough to accommodate the system loss in this link (the brief literature survey reported above shows losses that are lower than this power difference).

In conclusion, a careful system design for the on- and off-body links seems to be capable of accommodating the overall system requirements, hence, not being the key constraint for the implementation of this overall system.

IX. Conclusions

We have proposed a new diagnostic system based on implanted devices and nano-nodes circulating in the cardiovascular system. The system consists of bio-sensors and bio-actuators located in the pulmonary arteries, and a network of nano-nodes carried by the blood flow. A gateway node in the superior vena cava, and a subcutaneous node connected to a wearable devices are responsible to transfer the information out of the body and vice versa. The system elements communicate at THz band in its nano-network part and at GHz between the nano-gateway and the subcutaneous node transmitting to a wearable device, like a smartphone. The whole system enables two-way communications: from the bio-sensors reporting about possible cardiovascular issues to the external devices and, on the other hand, from the medical stuff to the internal bio-actuators, e.g. ordering the release of specific drugs. The proposed solution does not require a patient to be hospitalized, on contrary, it can be used by a person leading normal active life.

In this paper, we have focused on medical applications related to diseases of the vascular circulation system, which are one of the main causes of deaths in developed countries. We have addressed the issue of pulmonary blood circulation disorders, which can remain unnoticed by several days, at the same time being life threatening conditions. The delay in diagnosis of such disorders is known to be an important risk factor of fatal outcome.

Consequently, the performance of our proposed system has been evaluated in terms of diagnosis time and also the time of making a remote medical action, i.e., releasing specific drugs by bio-actuators. The values obtained from our analysis, about 3 h for the diagnosis (for 3^{rd} level artery blockage, and shorter in case of 2^{nd} or 1^{st} level occlusion) and another 3 h for releasing drugs without patient hospitalization, are very promising comparing with current practice and people with high risk of pulmonary disorders could strongly benefit from the presented solution.

While we have focused here on pulmonary disorders, the applications of the presented diagnostic system are not limited only to these problems. There are many other issues related to human vascular system, like tumor, bacterial and viral infections, sepsis and others, and in all these cases medicine can benefit from such a two-way communication system based on BANs and nano-networks providing tools for quick diagnosis and swift medical reaction.

Annex

A summary of all variables used in this paper together with their units is given in Table III.

Acknowledgement

This work was partially supported by the COST Action INTERACT under grant CA20120 and with a grant PID2020-116329GB-C22 funded by MCIN/AEI/10.13039/501100011033.

References

[1] Google Glass. Accessed: 2021-11-03. [Online]. Available: https://www.google.com/glass/start

[2] Ray-Ban. Accessed: 2021-11-03. [Online]. Available: https://www.ray-ban.com/usa/discover-ray-ban-stories/clp

[3] M. Patel and J. Wang, "Applications, challenges, and prospective in emerging body area networking technologies," *IEEE Wireless Communications*, vol. 17, no. 1, pp. 80–88, 2010.

[4] Y. A. Qadri, A. Nauman, Y. B. Zikria, A. V. Vasilakos, and S. W. Kim, "The future of healthcare internet of things: A survey of emerging technologies," *IEEE Communications Surveys & Tutorials*, vol. 22, no. 2, pp. 1121–1167, 2020.

[5] P. Kulakowski, K. Turbic, and L. M. Correia, "From nano-communications to body area networks: A perspective on truly personal communications," *IEEE Access*, vol. 8, pp. 159 839–159 853, 2020.

[6] F. Dressler and S. Fischer, "Connecting in-body nano communication with body area networks: Challenges and opportunities of the internet of nano things," *Nano Communication Networks*, vol. 6, no. 2, pp. 29–38, 2015.

[7] H. Rahmani and A. Babakhani, "A 1.6mm¡sup¿3¡/sup¿ wirelessly powered reconfigurable fdd radio with on-chip antennas achieving 4.7 pj/b tx and 1 pj/b rx energy efficiencies for medical implants," in *2020 IEEE Custom Integrated Circuits Conference (CICC)*, 2020, pp. 1–4.

[8] B. Jamali, S. Razavian, and A. Babakhani, "Fully electronic silicon-based THz pulse sources and detectors," in *Terahertz Photonics*, M. Jarrahi, S. Preu, and D. Turchinovich, Eds., vol. 11348, International Society for Optics and Photonics. SPIE, 2020, pp. 41 – 48.

[9] I. F. Akyildiz, M. Ghovanloo, U. Guler, T. Ozkaya-Ahmadov, A. F. Sarioglu, and B. D. Unluturk, "Panacea: An internet of bio-nanothings application for early detection and mitigation of infectious diseases," *IEEE Access*, vol. 8, pp. 140 512–140 523, 2020.

[10] H. Habibzadeh, K. Dinesh, O. Rajabi Shishvan, A. Boggio-Dandry, G. Sharma, and T. Soyata, "A survey of healthcare internet of things (hiot): A clinical perspective," *IEEE Internet of Things Journal*, vol. 7, no. 1, pp. 53–71, 2020.

[11] F. Alshehri and G. Muhammad, "A comprehensive survey of the internet of things (iot) and ai-based smart healthcare," *IEEE Access*, vol. 9, pp. 3660–3678, 2021.

[12] Y.-S. Su, T.-J. Ding, and M.-Y. Chen, "Deep learning methods in internet of medical things for valvular heart disease screening system," *IEEE Internet of Things Journal*, pp. 1–1, 2021.

[13] L. Sun, X. Jiang, H. Ren, and Y. Guo, "Edge-cloud computing and artificial intelligence in internet of medical things: Architecture, technology and application," *IEEE Access*, vol. 8, pp. 101 079–101 092, 2020.

[14] W. J. Powers, A. A. Rabinstein, T. Ackerson, O. M. Adeoye, N. C. Bambakidis, K. Becker *et al.*, "Guidelines for the Early Management of Patients With Acute Ischemic Stroke: 2019 Update to the 2018 Guidelines for the Early Management of Acute Ischemic Stroke: A Guideline for Healthcare Professionals From the American Heart Association/American Stroke Association," *Stroke*, vol. 50, no. 12, pp. e344–e418, 2019.

[15] S. V. Konstantinides, G. Meyer, C. Becattini, H. Bueno, G.-J. Geersing, V.-P. Harjola *et al.*, "2019 ESC Guidelines for the diagnosis and management of acute pulmonary embolism developed in collaboration with the European Respiratory Society (ERS): The Task Force for the diagnosis and management of acute pulmonary embolism of the European Society of Cardiology (ESC)," *European Heart Journal*, vol. 41, no. 4, pp. 543–603, 08 2019.

[16] J.-P. Collet, H. Thiele, E. Barbato, O. Barthélémy, J. Bauersachs, D. L. Bhatt *et al.*, "2020 ESC Guidelines for the management of acute coronary syndromes in patients presenting without persistent ST-segment elevation: The Task Force for the management of acute coronary syndromes in patients presenting without persistent ST-segment elevation of the European Society of Cardiology (ESC)," *European Heart Journal*, 08 2020.

[17] Eurostat. (2020) Causes and occurrence of deaths in the eu. Accessed: 2021-10-07. [Online]. Available: https://ec.europa.eu/eurostat/web/products-eurostat-news/-/ddn-20200721-1

[18] M. Arrigo and L. C. Huber, "Pulmonary embolism and heart failure: A reappraisal," *Cardiac Failure Review*, vol. 7, Feb. 2021.

[19] D. Siegal and W. Lim, "Chapter 142 - venous thromboembolism," in *Hematology (Seventh Edition)*, seventh edition ed., R. Hoffman, E. J. Benz, L. E. Silberstein, H. E. Heslop, J. I. Weitz, J. Anastasi *et al.*, Eds. Elsevier, 2018, pp. 2102–2112.

[20] D. R. Anderson and D. C. Barnes, "Computerized tomographic pulmonary angiography versus ventilation perfusion lung scanning for the diagnosis of pulmonary embolism," *Current Opinion in Pulmonary Medicine*, vol. 15, no. 5, pp. 425–429, Sep. 2009.

[21] K. R. Nilsson, J. P. Piccini, and M. D. C. Llc., *The Osler medical handbook*. Philadelphia, PA.: Mosby :;MD Consult, 2006.

[22] C. Wittram, A. C. Waltman, J.-A. O. Shepard, E. Halpern, and L. R. Goodman, "Discordance between CT and angiography in the PIOPED II study," *Radiology*, vol. 244, no. 3, pp. 883–889, Sep. 2007.

[23] P. D. Stein, "Gadolinium-enhanced magnetic resonance angiography for pulmonary embolism," *Annals of Internal Medicine*, vol. 152, no. 7, p. 434, Apr. 2010.

[24] S. Walen, R. A. Damoiseaux, S. M. Uil, and J. W. van den Berg, "Diagnostic delay of pulmonary embolism in primary and secondary care: a retrospective cohort study," *British Journal of General Practice*, vol. 66, no. 647, pp. e444–e450, 2016.

[25] Y. Bulbul, S. Ozsu, P. Kosucu, F. Oztuna, T. Ozlu, and M. Topbas, "Time delay between onset of symptoms and diagnosis in pulmonary thromboembolism," *Respiration*, vol. 78, no. 1, pp. 36–41, 2009.

[26] C. G. Elliott, S. Z. Goldhaber, and R. L. Jensen, "Delays in diagnosis of deep vein thrombosis and pulmonary embolism," *Chest*, vol. 128, no. 5, pp. 3372–3376, Nov. 2005.

[27] A. G. Bach, R. Bandzauner, B. Nansalmaa, N. Schurig, H. J. Meyer, B.-M. Taute *et al.*, "Timing of pulmonary embolism diagnosis in the emergency department," *Thrombosis Research*, vol. 137, pp. 53–57, 2016.

[28] B. Ibanez, S. James, S. Agewall, M. J. Antunes, C. Bucciarelli-Ducci, H. Bueno *et al.*, "2017 ESC Guidelines for the management of acute myocardial infarction in patients presenting with ST-segment elevation: The Task Force for the management of acute myocardial infarction in patients presenting with ST-segment elevation of the European Society of Cardiology (ESC)," *European Heart Journal*, vol. 39, no. 2, pp. 119–177, 08 2017.

[29] C. Caro, *The Mechanics of the Circulation*. Cambridge: Cambridge University Press, 2011.

[30] C. Stone, *Current diagnosis & treatment*. New York: McGraw-Hill Education, 2017.

[31] A. S. Ferrell, Y. J. Zhang, O. Diaz, R. Klucznik, and G. W. Britz, "Modern interventional management of stroke," *Methodist DeBakey Cardiovascular Journal*, vol. 10, no. 2, pp. 105–110, Apr. 2014.

[32] S. Canovas-Carrasco, A.-J. Garcia-Sanchez, F. Garcia-Sanchez, and J. Garcia-Haro, "Conceptual Design of a Nano-Networking Device," *Sensors*, vol. 16, no. 12, p. 2104, Dec. 2016.

[33] R. Asorey-Cacheda, S. Canovas-Carrasco, A.-J. Garcia-Sanchez, and J. Garcia-Haro, "An Analytical Approach to Flow-Guided Nanocommunication Networks," *Sensors*, vol. 20, no. 5, p. 1332, Feb 2020.

[34] S. Canovas-Carrasco, A.-J. Garcia-Sanchez, and J. Garcia-haro, "A nanoscale communication network scheme and energy model for a human hand scenario," *Nano Communication Networks*, vol. 15, pp. 17–27, Mar. 2018.

[35] K. Y. R. Kam, J. M. Mari, and T. J. Wigmore, "Adjacent central venous catheters can result in immediate aspiration of infused drugs during renal replacement therapy," *Anaesthesia*, vol. 67, no. 2, pp. 115–121, Nov. 2011.

[36] S. Canovas-Carrasco, A.-J. Garcia-Sanchez, and J. Garcia-Haro, "On the Nature of Energy-Feasible Wireless Nanosensor Networks," *Sensors*, vol. 18, no. 5, p. 1356, Apr. 2018.

[37] J. M. Jornet and I. F. Akyildiz, "Femtosecond-Long Pulse-Based Modulation for Terahertz Band Communication in Nanonetworks," *IEEE Transactions on Communications*, vol. 62, no. 5, pp. 1742–1754, 2014.

[38] S. Canovas-Carrasco, R. Asorey-Cacheda, A.-J. Garcia-Sanchez, J. Garcia-Haro, K. Wojcik, and P. Kulakowski, "Understanding the applicability of terahertz flow-guided nano-networks for medical applications," *IEEE Access*, vol. 8, pp. 214 224–214 239, 2020.

[39] R. Alsheikh, N. Akkari, and E. Fadel, "MAC protocols for Wireless Nano-sensor Networks: Performance analysis and design guidelines," in *2016 Sixth International Conference on Digital Information Processing and Communications (ICDIPC)*, 2016, pp. 129–134.

[40] J. M. Jornet, J. Capdevila Pujol, and J. Solé Pareta, "PHLAME: A Physical Layer Aware MAC protocol for Electromagnetic nanonetworks in the Terahertz Band," *Nano Communication Networks*, vol. 3, no. 1, pp. 74 – 81, 2012.

[41] Q. Xia, Z. Hossain, M. J. Medley, and J. M. Jornet, "A Link-layer Synchronization and Medium Access Control Protocol for Terahertz-band Communication Networks," *IEEE Transactions on Mobile Computing*, pp. 1–1, 2019.

[42] R. Chavez-Santiago, C. Garcia-Pardo, A. Fornes-Leal, A. Valles-Lluch, G. Vermeeren, W. Joseph *et al.*, "Experimental Path Loss Models for In-Body Communications within 2.36-2.5 GHz." *IEEE Journal of Biomedical and Health Informatics*, vol. 19, no. 3, pp. 930–937, 2015.

[43] P. Bose, A. Khaleghi, M. Albatat, J. Bergsland, and I. Balasingham, "RF Channel Modeling for Implant-to-Implant Commu-

nication and Implant to Subcutaneous Implant Communication for Future Leadless Cardiac Pacemakers," *IEEE Transactions on Biomedical Engineering*, vol. 65, no. 12, pp. 2798–2807, dec 2018.

[44] R. Chávez-Santiago, I. Balasingham, and J. Bergsland, "Ultrawideband technology in medicine: A survey," *Journal of Electrical and Computer Engineering*, vol. 2012, 2012.

[45] R. Chavez-Santiago, C. Garcia-Pardo, A. Fornes-Leal, A. Valles-Lluch, I. Balasingham, and N. Cardona, "Ultra wideband propagation for future in-body sensor networks," in *2014 IEEE 25th Annual International Symposium on Personal, Indoor, and Mobile Radio Communication (PIMRC)*. IEEE, 2014, pp. 2160–2163.

[46] C. Garcia-Pardo, A. Fornes-Leal, N. Cardona, R. Chavez-Santiago, J. Bergsland, I. Balasingham *et al.*, "Experimental ultra wideband path loss models for implant communications," in *2016 IEEE 27th Annual International Symposium on Personal, Indoor, and Mobile Radio Communications (PIMRC), Valencia*. IEEE, sep 2016, pp. 1–6.

[47] C. Garcia-Pardo, C. Andreu, A. Fornes-Leal, S. Castello-Palacios, S. Perez-Simbor, M. Barbi *et al.*, "Ultrawideband Technology for Medical In-Body Sensor Networks: An Overview of the Human Body as a Propagation Medium, Phantoms, and Approaches for Propagation Analysis," *IEEE Antennas and Propagation Magazine*, jun 2018.

[48] C. Andreu, C. Garcia-Pardo, A. Fomes-Leal, M. Cabedo-Fabres, and N. Cardona, "UWB in-body channel performance by using a direct antenna designing procedure," in *2017 11th European Conference on Antennas and Propagation, EUCAP 2017*, 2017.

[49] P. Bose, A. Khaleghi, and I. Balasingham, "In-Body and Off-Body Channel Modeling for Future Leadless Cardiac Pacemakers Based on Phantom and Animal Experiments," *IEEE Antennas and Wireless Propagation Letters*, vol. 17, no. 12, pp. 2484–2488, dec 2018.

[50] L. J. Xu, Y. X. Guo, and W. Wu, "Dual-band implantable antenna with open-end slots on ground," *IEEE Antennas and Wireless Propagation Letters*, vol. 11, pp. 1564–1567, 2012.

[51] F. Faisal, M. Zada, A. Ejaz, Y. Amin, S. Ullah, and H. Yoo, "A Miniaturized Dual-Band Implantable Antenna System for Medical Applications," *IEEE Transactions on Antennas and Propagation*, vol. 68, no. 2, pp. 1161–1165, feb 2020.

[52] J. Blauert, Y. S. Kang, and A. Kiourti, "In Vivo Testing of a Miniature 2.4/4.8 GHz Implantable Antenna in Postmortem Human Subject," *IEEE Antennas and Wireless Propagation Letters*, vol. 17, no. 12, pp. 2334–2338, dec 2018.

[53] E. Motovilova and S. Y. Huang, "A Review on Reconfigurable Liquid Dielectric Antennas," *Materials*, vol. 13, no. 8, p. 1863, apr 2020.

[54] S. G. Kirtania, A. W. Elger, M. R. Hasan, A. Wisniewska, K. Sekhar, T. Karacolak, and P. K. Sekhar, "Flexible antennas: A review," 2020.

[55] N. Tiercelin, P. Coquet, R. Sauleau, V. Senez, and H. Fujita, "Polydimethylsiloxane membranes for millimeter-wave planar ultra flexible antennas," *Journal of Micromechanics and Microengineering*, vol. 16, no. 11, pp. 2389–2395, nov 2006.

[56] C. W. Kim and T. S. P. See, "Rf transmission power loss variation with abdominal tissues thicknesses for ingestible source," in *2011 IEEE 13th International Conference on e-Health Networking, Applications and Services*, 2011, pp. 282–287.

[57] M. F. Awan, S. Perez-Simbor, C. Garcia-Pardo, K. Kansanen, P. Bose, S. Castelló-Palacios, and N. Cardona, "Experimental phantom-based evaluation of physical layer security for future leadless cardiac pacemaker," in *2018 IEEE 29th Annual International Symposium on Personal, Indoor and Mobile Radio Communications (PIMRC)*, 2018, pp. 333–339.

[58] J. Blauert and A. Kiourti, "Bio-matched horn: A novel 1–9 ghz on-body antenna for low-loss biomedical telemetry with implants," *IEEE Transactions on Antennas and Propagation*, vol. 67, no. 8, pp. 5054–5062, 2019.

[59] S. M. Asif, A. Iftikhar, J. W. Hansen, M. S. Khan, D. L. Ewert, and B. D. Braaten, "A novel rf-powered wireless pacing via a rectenna-based pacemaker and a wearable transmit-antenna array," *IEEE Access*, vol. 7, pp. 1139–1148, 2019.

[60] R. B. Green, M. Hays, M. Mangino, and E. Topsakal, "An anatomical model for the simulation and development of subcutaneous implantable wireless devices," *IEEE Transactions on Antennas and Propagation*, vol. 68, no. 10, pp. 7170–7178, 2020.

[61] *IEEE Standard for Local and Metropolitan Area Networks – Part 15.6: Wireless Body Area Networks*, IEEE Standard 802.15.6-2012, Feb. 2012.

[62] S. L. Cotton, "A Statistical Model for Shadowed Body-Centric Communications Channels: Theory and Validation," *IEEE Transactions on Antennas and Propagation*, vol. 62, no. 3, pp. 1416–1424, Mar. 2014.

[63] K. Turbic and L. M. Correia, "Effects On Polarization Characteristics of Off-Body Channels with Dynamic Users," in *Proc. IEEE Wireless Communications and Networking Conference (WCNC)*, Seoul, South Korea, Apr. 2020.

[64] S. L. Cotton, R. D'Errico, and C. Oestges, "A Review of Radio Channel Models for Body Centric Communications," *Radio Science*, vol. 49, no. 6, pp. 371–388, June 2014.

[65] G. Koutitas, "Multiple Human Effects in Body Area Networks," *IEEE Antennas and Wireless Propagation Letters*, vol. 9, pp. 938–941, Sep. 2010.

[66] T. Mavridis, L. Petrillo, J. Sarrazin, D. Lautru, A. Benlarbi-Delai, and P. De Doncker, "Theoretical and Experimental Investigation of a 60-GHz Off-Body Propagation Model," *IEEE Transactions on Antennas and Propagation*, vol. 62, no. 1, pp. 393–402, Jan. 2014.

[67] X. Huang, Y. Wu, F. Ke, K. Liu, and Y. Ding, "An Energy-Efficient and Reliable Scheduling Strategy for Dynamic WBANs With Channel Periodicity Exploitation," *IEEE Sensors Journal*, vol. 20, no. 5, pp. 2812–2824, Mar. 2020.

[68] S. L. Cotton and W. G. Scanlon, "Channel Characterization for Single- and Multiple-Antenna Wearable Systems Used for Indoor Body-to-Body Communications," *IEEE Transactions on Antennas and Propagation*, vol. 57, no. 4, pp. 980–990, Apr. 2009.

[69] K. Turbic, L. M. Correia, and M. Beko, "A Channel Model for Polarised Off-Body Communications with Dynamic Users," *IEEE Transactions on Antennas and Propagation*, vol. 67, no. 11, pp. 7001–7013, Nov. 2019.

[70] S.-C. Kwon, G. Stüber, A. Lopez, and J. Papapolymerou, "Geometrically Based Statistical Model for Polarized Body-Area-Network Channels," *IEEE Transactions on Vehicular Technology*, vol. 62, no. 8, pp. 3518–3530, Oct. 2013.

[71] ——, "Polarized Channel Model for Body Area Networks Using Reflection Coefficients," *IEEE Transactions on Vehicular Technology*, vol. 64, no. 8, pp. 3822–3828, Aug. 2015.

[72] K. Turbic, M. Särestöniemi, M. Hämäläinen, and L. M. Correia, "User Influence on Polarization Characteristics in Off-Body Channels," *IEEE Access*, vol. 8, pp. 167 570–167 584, Sep. 2020.

[73] L. Vallozzi, P. Van Torre, C. Hertleer, H. Rogier, M. Moeneclaey, and J. Verhaevert, "Wireless Communication for Firefighters Using Dual-Polarized Textile Antennas Integrated in Their Garment," *IEEE Transactions on Antennas and Propagation*, vol. 58, no. 4, pp. 1357–1368, Apr. 2010.

[74] P. V. Torre, L. Vallozzi, C. Hertleer, H. Rogier, M. Moeneclaey, and J. Verhaevert, "Indoor Off-Body Wireless MIMO Communication With Dual Polarized Textile Antennas," *IEEE Transactions on Antennas and Propagation*, vol. 59, no. 2, pp. 631–642, Feb. 2011.

[75] P. F. Cui, W. J. Lu, Y. Yu, B. Xue, and H. B. Zhu, "Off-Body Spatial Diversity Reception Using Circular and Linear Polarization: Measurement and Modeling," *IEEE Communications Letters*, vol. 22, no. 1, pp. 209–212, Jan. 2018.

[76] K. Turbic and L. M. Correia, "Influence of User Dynamics on Small-Scale Fading Characteristics in Off-Body Channels," in *Proc. IEEE International Conference on Communications (ICC)*, Dublin, Ireland, Jun. 2020.

[77] S. Canovas-Carrasco, R. Asorey-Cacheda, A. Garcia-Sanchez, J. Garcia-Haro, P. Kulakowski, and K. Wojcik, "A perfor-

mance evaluation of an in-body nano-network architecture," in *2020 IEEE 21st International Conference on High Performance Switching and Routing (HPSR)*, 2020, pp. 1–5.

[78] M. F. Awan, S. Perez-Simbor, C. Garcia-Pardo, K. Kansanen, and N. Cardona, "Experimental Phantom-Based Security Analysis for Next-Generation Leadless Cardiac Pacemakers," *Sensors*, dec 2018.

[79] S. Castello-Palacios, C. Garcia-Pardo, A. Fornes-Leal, N. Cardona, and A. Valles-Lluch, "Full-spectrum phantoms for cm-wave and medical wireless communications," in *IET Conference Publications*, 2018.

[80] S. Perez-Simbor, C. Andreu, C. Garcia-Pardo, M. Frasson, and N. Cardona, "UWB Path Loss Models for Ingestible Devices," *IEEE Transactions on Antennas and Propagation*, aug 2019.

[81] P. Bose, A. Khaleghi, S. Mahmood, M. Albatat, J. Bergsland, and I. Balasingham, "Evaluation of data telemetry for future leadless cardiac pacemaker," *IEEE Access*, vol. 7, pp. 157 933–157 945, 2019.

Rafael Asorey-Cacheda received his M.Sc. degree in Telecommunication Engineering (major in Telematics and Best Master Thesis Award) and his Ph.D. (cum laude and Best PhD Thesis Award) in Telecommunication Engineering from the Universidade de Vigo, Spain, in 2006 and 2009, respectively. He was a researcher with the Information Technologies Group, University of Vigo, Spain until 2009. Between 2008 and 2009 he was also R&D Manager at Optare Solutions, a Spanish telecommunications company. Between 2009 and 2012, he held an Ángeles Alvariño position, Xunta de Galicia, Spain. Between 2012 and 2018, he was an associate professor at the Centro Universitario de la Defensa en la Escuela Naval Militar, Universidade de Vigo. Currently, he is an associate professor at the Universidad Politécnica de Cartagena. He is author or co-author of more than 60 journal and conference papers, mainly in the fields of switching, wireless networking and content distribution. He has been a visiting scholar at New Mexico State University, USA (2007-2011) and at Universidad Politécnica de Cartagena, Spain (2011, 2015). His interests include content distribution, high-performance switching, peer-to-peer networking, wireless networks, and nano-networks.

Luis M. Correia (S'85–M'91–SM'03) was born in Portugal, in 1958. He received the Ph.D. in Electrical and Computer Engineering from IST (Univ. Lisbon) in 1991, where he is currently a Professor in Telecommunications, with his work focused on Wireless and Mobile Communications, with the research activities developed in the INESC-ID institute. He has acted as a consultant for the Portuguese telecommunications operators and regulator, besides other public and private entities, and has been in the Board of Directors of a telecommunications company. He has participated in 32 projects within European frameworks, having coordinated 6 and taken leadership responsibilities at various levels in many others, besides national ones. He has supervised over 220 M.Sc./Ph.D. students, having edited 6 books, contribute to European strategic documents, and authored over 500 papers in international and national journals and conferences, for which served also as a reviewer, editor and board member. Internationally, he was part of 37 Ph.D. juries, and 74 research projects and institutions evaluation committees for funding agencies in 12 countries, and the European Commission and COST. He has been the Chairman of Conference, of the Technical Programme Committee and of the Steering Committee of 25 major conferences, besides other several duties. He was a National Delegate to the COST Domain Committee on ICT. He has launched and served as Chairman of the IEEE Communications Society Portugal Chapter, besides being involved in several other duties in this society at the global level. He is an Honorary Professor of the Gdańsk University of Technology (Poland) and a recipient of the 2021 EurAAP Propagation Award "for leadership in the field of propagation for wireless and mobile communications".

Concepcion Garcia-Pardo attended the Universidad Politécnica de Cartagena (UPCT), where she received the Telecommunication Engineering degree in 2007 and the M.Sc. in Information Technologies and Communications in 2008. In 2012, she got her Ph.D. degree with European mention and qualification cum laude, from the UPCT, and Ph.D. degree in Microwaves and Microtechnologies with qualification Très Honorable from the Lille 1 University (USTL). Her Ph.D. Thesis was awarded the special prize from the UPCT in 2013.

In 2012, she joined the Institute of Telecommunications and Multimedia Applications (iTEAM) of the Universitat Politècnica de Valencia (UPV), Spain, where she is currently senior researcher. She is author of more 50 publications of journal and conference papers related to wireless communications. She has also participated in several national and international project related to wireless communications and wireless medical devices. She was also part of the management committee of COST Action CA 15104-IRACON. She was workshop chair at IEEE PIMRC 2018, and TPC Chair in IEEE ISMICT 2019 and IEEE HealthComm 2019. Her current work is focused on wireless medical devices and wireless communications for body area networks, as well as dielectric characterization of human body tissues.

Krzysztof Wójcik received his M.Sc. and Ph.D. degrees in biophysics from Jagiellonian University in 2003 and 2015, respectively, and an M.D. from Jagiellonian University Medical College (JUMC), Krakow, Poland,in 2007. He was an assistant in the Division of Cell Biophysics Faculty of Biochemistry, Biophysics and Biotechnology, Jagiellonian University (2007-2014). He is an assistant professor at the Department of Allergy, Autoimmunity and Hypercoagulability in II Chair of Internal Medicine JUMC. His research interest is focused on vasculitis and super-resolution microscopy techniques for auto-antibody detection. He is involved in European vasculitis research - FAIRVASC a Horizon 2020 funded project.

Kenan Turbic (S'16–M'19) received an MSc degree from the University of Sarajevo in 2011, and a PhD degree (Hons.) in Electrical and Computer Engineering from IST, University of Lisbon, in 2019. He was a postdoctoral research fellow at the INESC-ID research institute, Lisbon, Portugal, and currently he is a postdoctoral researcher at the Chair for Distributed Signal Processing, ICE, RWTH Aachen University, Aachen, Germany. He was actively participating in the COST Action CA15104 (IRACON), to which he contributed with several technical documents and served as one of the Section editors for the final report book. His main research interests include channel modeling and estimation, and signal processing for wireless communications.

Pawel Kulakowski received Ph.D. in telecommunications from the AGH University of Science and Technology in Krakow, Poland, in 2007, and currently he is working there as an assistant professor. In 2008-2013, he spent over 2 years in total as a post-doc or a visiting professor at Technical University of Cartagena, University of Girona, University of Castilla-La Mancha and University of Seville. He was involved in European research projects, serving in the Management Committees of COST Actions: IC1004, CA15104 IRACON, and CA20120 INTERACT, focusing on topics of nano-networking, wireless sensor networks, indoor localization and wireless communications in general. In 2019-2021, he was also an R&D manager for a national research project on 5G network planning. His current research interests include nano-networks and AI applications in medicine. He was recognized with several scientific distinctions, including 3 awards for his conference papers and a governmental scholarship for young outstanding researchers.

TABLE III: List of all variables used in the model.

Var.	Description
D_{cyl}	Flow diameter [m].
d	Distance [m].
d_0	Reference distance [m].
d_{mm}	Radius of the gateway coverage zone [m].
d_{nn}	Distance travelled by the nano-node [m].
$E_{b=0}$	Energy required to transmit or receive a 0 bit symbol [J].
$E_{b=1}$	Energy required to transmit or receive a 1 bit symbol [J].
$E_{f,max}$	Maximum energy required to transmit or receive a frame [J].
$f_{cha}(t)$	Nano-node charging frequency as a function of time [Hz].
$\overline{f_{cha}}$	Average nano-node charging frequency [Hz].
L_p	Path Loss [dB].
L_0	Path Loss at reference distance[dB].
N	Number of uniformly distributed nano-nodes in the flow-guided nano-network.
N_θ	Number of nano-nodes that maximizes throughput.
$p_{a,m}$	Probability of successfully activating a nano-actuator in round m.
p_{cv}	Probability of a nano-node being in the coverage zone of a nano-gateway or a bio-sensor/actuator.
p_{cx}	Probability of a nano-node being in the collision zone.
$p_{d,\tau,\epsilon}$	Probability for the nano-gateway of receiving a frame before ϵ time units if a nano-node remembers a bio-sensor frame reception for τ time units.
p_f	Probability of not detecting a bio-sensor in a time slot.
$p_{f,\tau}$	Probability of not detecting a bio-sensor after τ time slots.
$p_{Q,a}$	Probability of a bio-actuator gets activated.
$p_{Q,d}$	Probability of no false blocked artery detection is performed.
$p_{rx,T}$	Probability of a nano-node receiving a frame from a bio-sensor in a round.
$p_{rx,T,\tau}$	Probability of a nano-node receiving at least one frame from a bio-sensor after τ rounds.
p_{tx}	Probability of a nano-node being in the transmission zone.
$P_{rx\ min}$	Nano-gateway receiver sensitivity [W].
P_{tx}	Nano-node transmission power [W].
Q	Energy that can be stored by a nano-node [J].
R	Nano-node transmission rate [bit/s].
$\overline{r_{T,av}}$	Average number of successful frames by the nano-nodes during a round.
$T_{cha}(t)$	Time required by a nano-node to complete a round in the flow-guided network [s].
$\overline{T_{cir}}$	Average time required by a nano-node to complete a round in the flow-guided network [s].
t_f	Time required to transmit a frame [s].
t_p	Duration of the electromagnetic pulses in the On-Off Keying modulation [s].
$\overline{v}$	Average speed of the nano-node in the nano-gateway, bio-sensor, or bio-actuator coverage zone [m/s].
V_{cv}	Volume of the nano-gateway, bio-sensor, or bio-actuator coverage zone [m^3].
V_{cx}	Volume of the nano-gateway collision zone [m^3].
V_{net}	Flow-guided nano-network volume [m^3].
V_{rx}	Volume of the bio-sensor reception zone [m^3].
V_{tx}	Volume of the nano-gateway transmission zone [m^3].
α_{lin}	Channel path loss linear coefficient [dB/m].
α_{log}	Channel path loss log coefficient.
ϕ	Number of rounds for activation of the bio-actuator.
λ_d	Size of the frame data payload [B].
λ_f	Size of the frame [B].
λ_h	Size of the frame header addressing field [B].
λ_o	Size of other fields the frame [B].
σ	Standard deviation.
θ	Flow-guided nano-network throughput [bit/s].